

# A multifidelity framework for grey-box modelling of automated welding processes

M. B. Dodt<sup>1,2</sup>, L. Bogaerts<sup>1,2</sup>, A. Persoons<sup>1,2</sup>, M. G. R. Faes<sup>3</sup>, D. Moens<sup>1,2</sup>

<sup>1</sup> KU Leuven, Department of Mechanical Engineering,  
Jan Pieter de Nayerlaan 5, 2860 Sint-Katelijne-Waver, Belgium

<sup>2</sup> Flanders Make @ KU Leuven,  
Belgium

<sup>3</sup> TU Dortmund University, Chair for Reliability Engineering  
Leonhard-Euler-Strasse 5, 44227 Dortmund, Germany

## Abstract

Reliable monitoring for fast manufacturing processes, such as resistance spot welding is quite challenging in the face of uncertainties, process drift and long model evaluation times. It is however an essential basis to perform adequate control and receiving good output quality consistently. In the face of noisy data and slow-to-evaluate finite element models, that are magnitudes slower than the process itself, grey-box model offer a solution that is well suited for uncertainty quantification and addressing process drift. In particular, the authors look at a nested multifidelity model, which is easy to implement into a control loop and offers benefits of incorporating prior knowledge gained from a numerical model of the process as well as live process data. A simple electric heating equation is studied to compare the predictability and performance of single-fidelity models with two high-fidelity models. The model is further affected by process drift as well as measurement and input uncertainties.

## 1 Introduction

Resistance spot welding is a manufacturing process that is important in many industrial fields, such as car and battery production. In a good car body production line, for example, more than seven million welds are produced a day with a single vehicle containing about 2000 to 5000 individual spot welds [1]. Two to three thin metal plates are joint locally by sending through high electrical current (kA) for a short amount of time (40-400ms) [2]. The resistance between the metal sheets is large, generating heat, which in turn melts the sheets. The highly dynamic process is greatly affected by noise and uncertainties, as well as an unpredictable and difficult to quantify process drift. The process drift is mainly caused by electrode wear [3]. Over time, dirt accumulates on the electrodes and the electrode deforms and flattens. After a threshold has been met, the electrodes need to be milled down. Milling the electrodes decreases the weight and thickness thereof. This process significantly impacts the internal resistance – both overall and in the contribution of its individual components, including the resistance of the electrode, the electrode-to-plate interface, and between plates – which plays a key role in heat generation and output quality. It is further clear, that after a certain number of the so-called dressings, the electrode head needs to be exchanged [3]. The electrode but also the machine itself and the material are all affected by uncertainty and minor changes from one weld to the next. This leads to significant uncertainties in the process and controlling the output quantity reliably becomes an important challenge.

The challenges to achieve robust and satisfactory welding results are similar to those in other manufacturing processes. There are three main challenges to address. One control challenge lies in the dynamics of

the process. Resistance spot welding is a fast process, which takes only between 40 and 400 milliseconds. Modelling the complex physics with a white-box model, such as a finite element model, results in evaluation times magnitudes larger than the process itself, therefore prohibiting process control based on a FE model alone. Previously, various black-box and grey-box modelling approaches have been proposed to tackle this challenge [1, 4, 5, 6]. The second challenge concerns the uncertainty quantification of the process, which is paramount to produce high quality output consistently and reliably. Many grey-box modelling approaches inherently perform uncertainty quantification and provide an estimation about the reliability of their own prediction [7]. Finally, the third challenge is the quantification of the process drift. Some parameters that cannot be controlled, such as the electrode wear, can greatly affect the output quantity. This effect is difficult to predict and to quantify. It is assumed, that the drift cannot be modelled by a finite element model or white-box model but that noisy measurements of the output quantity reflect its effect.

The control performed needs to be robust against the presented challenges, which in turn requires that the monitoring, including data processing, properly addresses the uncertainty quantification, drift and process state assessment as well as the time-scale-discrepancy.

In summary, to generate a consistently satisfactory output quantity, it is indispensable to address the presented challenges. This can be done by creating a reliable, fast-to-evaluate model that can further cope with process drift and noisy measurement data. The authors propose a grey-box model including a multifidelity framework which can be easily incorporated into a control flow. A multifidelity model joins information gained from models with different fidelities, in other words accuracy. In this model, noisy measurement data are seen as the high-fidelity model and a finite element output is assumed to be the low-fidelity model. The methodology presented is modular and can deal well with uncertainty and noise, which makes it versatile and highly adaptable. An analytical example is presented to test in which cases the process drift can or cannot be evaluated satisfactorily.

## 2 Methodology

In multifidelity modelling, two or more models of different fidelity are joined. Usually, the goal is to decrease computation time while increasing the accuracy by combining a fast but less accurate model with an accurate but computational expensive model. There are two main approaches to multifidelity: the parallel approach and the nested approach. In the parallel approach it is decided which model to evaluate at each step individually [8]. In the nested approach however, each high-fidelity model contains its next-lower fidelity model. For the latter, a clear hierarchy is of importance.

In this paper, a nested approach, based on the work of Giannoukou et al. [9] is used for its simplicity and general applicability. It is assumed, that the high-fidelity model  $\mathcal{M}_{HF}$  can be expressed as the sum of the scaled low-fidelity model  $\mathcal{M}_{LF}$  and a discrepancy term  $\delta$

$$\mathcal{M}_{HF} = \rho \cdot \mathcal{M}_{LF} + \delta. \quad (1)$$

The constant scaling coefficient  $\rho$  can be estimated through

$$\hat{\rho} = \mathbb{E} \left[ \frac{y_{HF}(\mathbf{x}_{HF})}{\mathcal{M}_{LF}(\mathbf{x}_{HF})} \right] \approx \frac{1}{n_{HF}} \cdot \sum_{i=1}^{n_{HF}} \frac{y_{HF}(\mathbf{x}_{HF}^{(i)})}{\mathcal{M}_{LF}(\mathbf{x}_{HF}^{(i)})} \quad (2)$$

with the hat-accent indicating an estimation [9]. The high-fidelity evaluations of the sampling points  $\mathbf{x}_{HF}^{(i)}$  are denoted by  $y_{HF}$ . Rearranging eq. 1 gives the following expression of an estimation of the discrepancy  $\hat{\delta}$

$$\hat{\delta} = y_{HF}(\mathbf{x}_{HF}) - \hat{\rho} \cdot \mathcal{M}_{LF}(\mathbf{x}_{HF}). \quad (3)$$

In the next step, a surrogate model is trained on the discrepancy. Here both a polynomial chaos expansion (PCE) surrogate model [10] as well as a Kriging regression model [11] have been trained. Both methods are

long established, well suitable for active learning [12, 13, 14], as they provide the advantage of being able to assess their own reliability. PCE additionally provides variance-based sensitivity analysis for free [10]. In the case of more than two fidelity levels, the described process can be repeated as often as necessary. Further, it is possible to exchange the low-fidelity model with a surrogate model trained on low-fidelity data, in cases of limited data-availability or reducing computational costs.

### 3 Case study

In this case study a simple function relevant to welding is looked at: the Joule heating, also called Ohmic or resistive heating. Equation 4 describes the heat generated by electric current  $Q$

$$Q = I^2 \cdot R \cdot t \quad (4)$$

with the current  $I$ , resistance  $R$  and total welding duration  $t$  of each singular weld. What is referred to as the total welding duration means in essence the time the current flows and a heat source is thus active. As it was explained in the introduction, welding is a highly complex process and this simple equation does not capture its complexity. It covers however a relevant part of the welding process is suitable to study whether multifidelity modelling is capable of capturing the process drift and predicting the outputs accordingly. This example was further chosen to have access to the noise-free ground truth function  $f_{GT}$  to compare the results with.

The heat equation is corrupted with noise and process drift affects the resistance. In the case study, two noise level were examined and the available high-fidelity data-points were varied between 5 and 70.

#### 3.1 Noisy welding process model

To more realistically mimic the welding process, it is assumed, that the user-input current  $I_u$  arrives in the machine with slight deviations

$$I = I_u + \varepsilon_1 \quad \text{with } \varepsilon_1 \sim \mathcal{N}(0, \sigma_1 \cdot I_u), \quad (5)$$

whereas the time is not affected by process uncertainties. The noise-term  $\varepsilon_1$  is unbiased normal-distributed with  $\sigma_1$  of 0.1 % of the current for minor or respectively 1 % for major noise.

The resistance  $R$  is affected by material stochasticity and process drift. It is assumed, that

$$R = a^{k \cdot b} \quad (6)$$

describes the general drift behaviour of the resistance. It is classified by the basis  $a$  with  $1 < a < 2$ , which is affected by noise with  $a \sim \mathcal{N}(a_0, \sigma_a)$ , and exponent  $b$ , which is a scalar to scale the growth. We assume in general  $b < 1$  and  $a$  close to 1, which translates to a moderate growth of the internal resistance  $R$ . The progression of the drift is described by  $\{k \in \mathbb{R} : k \geq 0\}$ .  $k = 0$  refers to a drift-free state. The larger  $k$ , the larger is the impact of the drift. In a measurement campaign,  $k$  could represent the process number or the sequence position of the process.

Similarly to the welding case, it is assumed, that the current  $I_m$  and voltage  $V_m$  can be measured during the process. Both are affected by an unbiased noise of about  $\varepsilon_2$  or  $\varepsilon_3$  respectively. This gives

$$I_m = I + \varepsilon_2 \quad \text{with } \varepsilon_2 \sim \mathcal{N}(0, \sigma_2 \cdot I) \quad (7)$$

for the measured current and

$$V_m = V + \varepsilon_3 \quad \text{with } \varepsilon_3 \sim \mathcal{N}(0, \sigma_3 \cdot V) \quad (8)$$

for the voltage. The true voltage  $V$  can be computed from the ground-truth resistance  $R_{gt}$  and the current  $I$  by

$$V = R_{gt} \cdot I. \quad (9)$$

The ground-truth function, which should be recreated through the modelling strategies, is then described by

$$f_{GT} = I^2 \cdot R \cdot t = [I_u + \varepsilon_1]^2 \cdot [a^{k \cdot b}] \cdot t_u. \quad (10)$$

The low-fidelity function is uninformed about the process drift and takes user inputs denoted by subscript  $u$ . It is described by

$$f_{LF} = I_u \cdot \bar{R} \cdot t_u \quad (11)$$

with the mean resistance  $\bar{R}$ .

During the resistance spot welding process, it is possible to measure the current  $I_m$  as well as the voltage  $V_m$ . Both values, as well as the user-chosen welding duration  $t_u$  and the drift state  $k$  are available for training the black-box model and the multifidelity model. The output for the training data is given by

$$f_{HF} = f_{GT} + \varepsilon_4, \quad (12)$$

by assuming that it is measured, hence noisy.

The analytical example was run for two different noise levels, each for six different levels of high-fidelity data availability  $n_{HF}$ , each repeated 100 times for two single-fidelity models and two multifidelity models. The single-fidelity models are, one, the low-fidelity, analytical function (LFM), which is uninformed about the processes drift and two, a black-box model (BBM), trained on the high-fidelity data alone. The multifidelity models are both using the scheme presented in the previous chapter, one with polynomial chaos expansion as the surrogate model for  $\hat{\delta}$ , the second with a Kriging regression model. All of these models were created using UQLab [15] in Matlab.

Table 1 gives an overview over the range and distribution of the considered parameters with table 2 providing necessary additional information to table 1.

Table 1: Overview over sampling range of parameters.

Parameters	Range	Distribution
Current $I_u$	[4, 12]	Uniform
Duration $t$	[100, 400]	Uniform
Drift indicator parameter $k$	[1, 100]	Uniform
$a$	(1.01, $\sigma_a$ )	Normal
Machine error on $I$ $\varepsilon_1$	(0, $\sigma_1 \cdot I_u$ )	Normal
Measurement error on $I$ $\varepsilon_2$	(0, $\sigma_2 \cdot I$ )	Normal
Measurement error on $V$ $\varepsilon_3$	(0, $\sigma_3 \cdot V$ )	Normal
Measurement error on output $\varepsilon_4$	(0, $\sigma_4 \cdot I$ )	Normal

Table 2: Overview over additional relevant parameters.

Parameters	Values
$b$	0.8
$\sigma_a$	0.001 and 0.01
$\sigma_1$	0.01 and 0.05
$\sigma_2$	0.005 and 0.025
$\sigma_3$	0.005 and 0.025
$\sigma_4$	0.01 and 0.05
$n_{HF}$	5, 10, 20, 35, 50, 70

### 3.2 Results

Figure 1 shows the distribution of the R2-value, the coefficient of determination for the case of small noise and figure 2 respectively for the larger noise. The R2-value is computed on the basis of the noise-free ground truth values through the following equation:

$$R2 = 1 - \frac{\sum_i (y_{gt,i} - f_i)^2}{\sum_i (y_{gt,i} - \bar{y}_{gt})^2} \quad (13)$$

with  $f_i$  as the  $i$ -th result of either model, the low-fidelity model (LFM), black-box model (BBM), PCE multifidelity model (PCE-MFM) or Kriging regression multifidelity model (KR-MFM). Tables 3 and 4 provide the mean R2-value over 100 realisations for each of the four models for each level of high-fidelity samples.

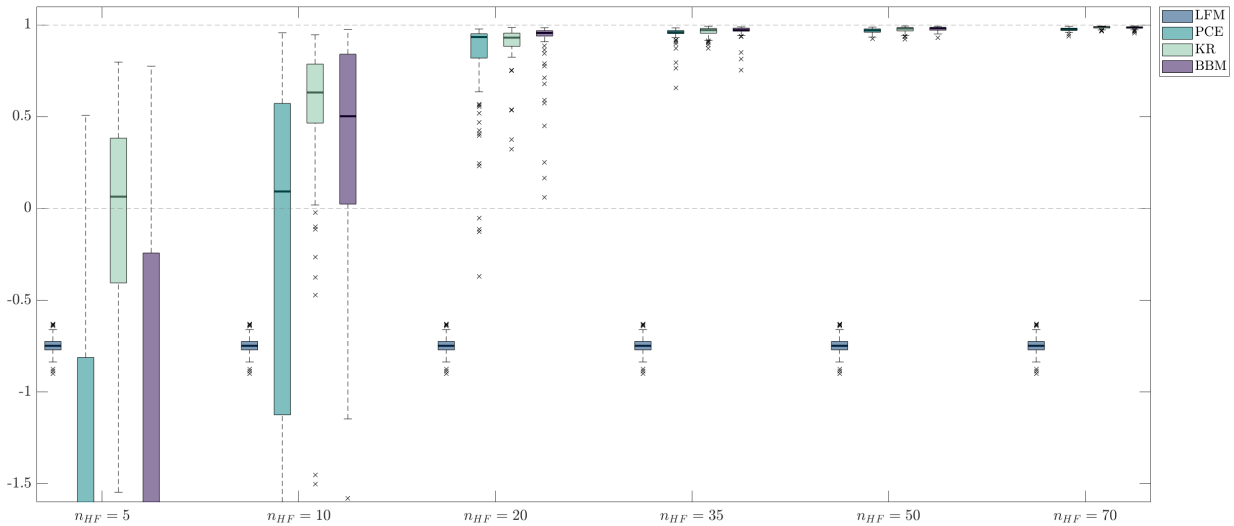


Figure 1: Boxplot of the coefficient of determination for the 4 methods over 100 realisations each for 6 different level of high-fidelity data availability - little noise present.

For both noise-levels negative R2-values can be observed for the case of a black- or grey-box model with a low number of high-fidelity data-points and the low-fidelity model. A negative R2-value means that the model fits the data worse than any ordinary least-squares predictors and points to nonsensical constraints applied or a wrong model used. It can be observed, that in the case of grey- and black-box models, this can also point to too few high-fidelity data-points to have a significant correlation and to create a meaningful model.

Table 3: Mean coefficient of determination in the presence of minor noise.

Model	$n_{HF} = 5$	$n_{HF} = 10$	$n_{HF} = 20$	$n_{HF} = 35$	$n_{HF} = 50$	$n_{HF} = 70$
BBM	-13.711	0.1355	0.909	0.968	0.979	0.985
PCE-MFM	-24.412	-1.360	0.817	0.952	0.968	0.986
KR-MFM	-0.413	0.495	0.901	0.964	0.976	0.986
LFM	-0.750					

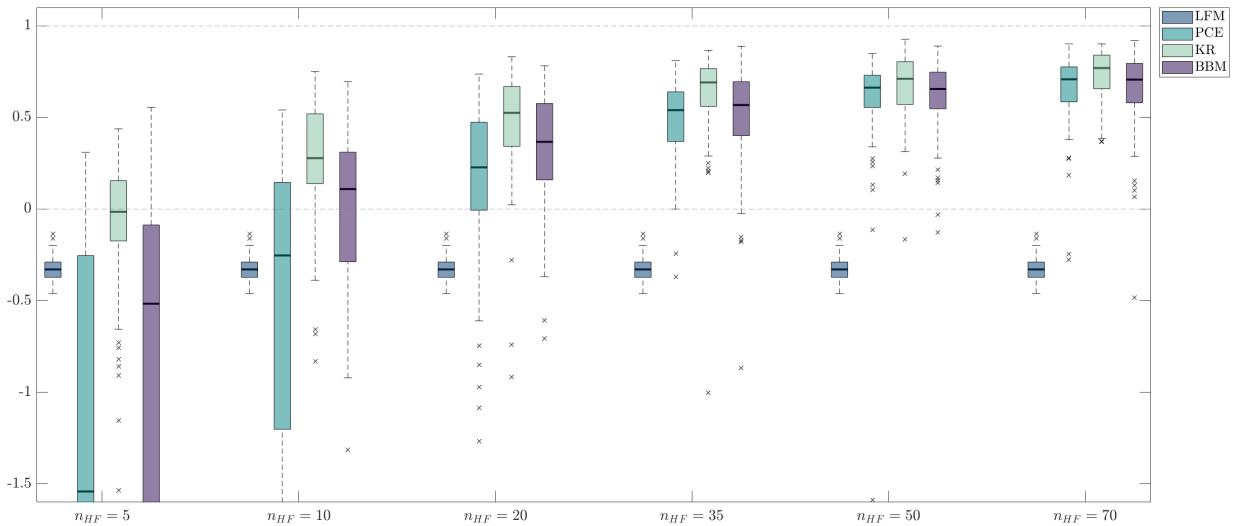


Figure 2: Boxplot of the coefficient of determination for the 4 methods over 100 realisations each for 6 different level of high-fidelity data availability - more noise present.

Table 4: Mean coefficient of determination in the presence of major noise.

Model	$n_{HF} = 5$	$n_{HF} = 10$	$n_{HF} = 20$	$n_{HF} = 35$	$n_{HF} = 50$	$n_{HF} = 70$
BBM	-4.110	-0.169	0.237	0.479	0.612	0.658
PCE-MFM	-15.823	-0.912	0.075	0.420	0.598	0.659
KR-MFM	-0.183	0.267	0.475	0.633	0.672	0.731
LFM	1.325					

It is visible, that the low-fidelity model does not converge with an increased number of high-fidelity samples, because it is only calibrated on low-fidelity data and independent of the high-fidelity data-points. As it does not contain any information about the process drift, adding more LF-data points is fruitless. In this case, it can be said, that the model is not sufficient on its own.

The other three models converge with increasing number of high-fidelity samples. Furthermore, it is visible, that the less noise there is, the faster the convergence and the smaller the range of predictions. In the case of minor noise, all three methods converge quickly to an R2 value close to 1. In the presence of larger noise however, the convergence is slower and it is more difficult to guarantee their convergence to one. This is a common problem for very noisy cases, where a certain noise-floor is difficult to eradicate within a finite number of samples.

As can be seen in table 4, convergence has not been reached within 70 high-fidelity data-points for BBM, PCE-MFM and KR-MFM. More data would be needed. Suppose, an R2-value greater than 0.8 can be reached with  $n_{HF} = 100$ , the model's accuracy might suffice in cases of limited HF-data availability, limited resources or as a first approximation.

Comparing BBM, PCE-MFM and KR-MFM with each other, it is observed, that the Kriging multifidelity model performs best in each case. It is the only methodology whose mean prediction is only barely negative for 5 HF-samples and already positive for 10 HF-samples. It also shows the fastest convergence rate. The PCE-BBM outperforms the PCE-MFM when limited high-fidelity data is available, but both converge to similar values as the amount of high-fidelity data increases. In other words, when high-fidelity data is plentiful, their performance becomes comparable, and the impact of the LF-model diminishes. This suggests, that – not surprisingly – a poor LF-model does more harm than good for multifidelity modelling.

From the available data, it cannot be clearly stated, that multifidelity modelling outperforms the black-box model in this case.

## 4 Conclusion

In this paper, a nested multifidelity scheme was employed to predict and assess with process drift. The scheme presented is well suited for application process control and digital twins because it can speed up evaluation and has some physical background to base its prediction on. Furthermore, it is simple to employ and allows the integration of various fidelity levels. Its key feature lies in training a surrogate on the discrepancy between the high-fidelity data-points and the low-fidelity predictions. Here, two different methods, Kriging regression and Polynomial Chaos Expansion, were chosen to create the surrogate model. Their performance was compared to the performance of the low-fidelity and data-driven model on an analytical case study.

Kriging regression MFM performed significantly better in the specific example than the PCE multifidelity model but previous studies indicate, that this might be influenced by the example chosen. The former outperformed the data-driven model, which was not the case for PCE-MFM. In the case of good availability of high-fidelity data, the performance of the presented multifidelity models is quite similar to the black-box model.

The chosen low-fidelity function did not capture one of the key trends: the process drift. This led to a worse performance for the PCE-MFM when only a small number of high-fidelity data-points were available. The authors suggest to first study the eligibility of the low-fidelity model before employing it. It is suggested, to use a low-fidelity model with a positive coefficient of determination.

The authors nevertheless believe, that grey-box modelling carries advantages over purely data-based models and that multifidelity modelling can be highly beneficial in digital twins when certain criteria have been fulfilled. One such criterion is, that the low-fidelity function should carry relevant information not contained in the high-fidelity model.

One such advantage is, that using Kriging regression or Polynomial Chaos regression as the surrogate model to estimate  $\hat{\delta}$  enables active learning in order to find the optimal set of high-fidelity samples that minimises the costs. Extending the current framework with active learning is for future work. As a closing remark, PCE and Kriging surrogate modelling are not well suited to perform transfer learning, which might be relevant for cases with no data availability. In these cases, another surrogate modelling technique, such as autoregressive models are suggested.

To conclude, multifidelity modelling is capable of capturing the process drift. However, so is the data-based model. In order for multifidelity modelling to outperform black-box modelling, the low-fidelity model needs to offer information that cannot be easily captured by the data available. If the low-fidelity model only performs worse with not additional knowledge gained, it might instead negatively effect the multifidelity performance. The method presented is efficient and straightforward, requiring only the additional low-fidelity model evaluations. Given its low-risk, high-reward potential, it is a strategy worth persuing, even if the benefits are not immediately apparent.

## Acknowledgements

This project has received funding from the European Union's Horizon 2020 Research and Innovation programme in the project GREYDIENT under grant agreement n°955393.

## References

- [1] K. Zhou and P. Yao, "Overview of recent advances of process analysis and quality control in resistance spot welding," *Mechanical Systems and Signal Processing*, vol. 124, pp. 170–198, Jun. 2019.
- [2] A. O'Brien and American Welding Society, Eds., *Welding handbook. Vol. 3: Welding processes, part 2 / Annette O'Brien, ed*, 9th ed. Miami, Fla: American Welding Soc, 2007, vol. 3.
- [3] C. Mathiszik, D. Köberlin, S. Heilmann, J. Zschetzsche, and U. Füssel, "General Approach for Inline Electrode Wear Monitoring at Resistance Spot Welding," *Processes*, vol. 9, no. 4, p. 685, Apr. 2021, number: 4 Publisher: Multidisciplinary Digital Publishing Institute.
- [4] W. Kritzing, M. Karner, G. Traar, J. Henjes, and W. Sihn, "Digital Twin in manufacturing: A categorical literature review and classification," *IFAC-PapersOnLine*, vol. 51, no. 11, pp. 1016–1022, 2018.
- [5] X. Wan, Y. Wang, and D. Zhao, "Quality monitoring based on dynamic resistance and principal component analysis in small scale resistance spot welding process," *The International Journal of Advanced Manufacturing Technology*, vol. 86, no. 9-12, pp. 3443–3451, Oct. 2016.
- [6] L. Zhou, T. Li, W. Zheng, Z. Zhang, Z. Lei, L. Wu, S. Zhu, and W. Wang, "Online monitoring of resistance spot welding electrode wear state based on dynamic resistance," *Journal of Intelligent Manufacturing*, vol. 33, no. 1, pp. 91–101, Jan. 2022.
- [7] L. Bogaerts, A. Dejans, M. G. R. Faes, and D. Moens, "A machine learning approach for efficient and robust resistance spot welding monitoring," *Welding in the World*, vol. 67, no. 8, pp. 1923–1935, 2023.
- [8] B. Peherstorfer, K. Willcox, and M. Gunzburger, "Survey of Multifidelity Methods in Uncertainty Propagation, Inference, and Optimization," *SIAM Review*, vol. 60, no. 3, pp. 550–591, Jan. 2018.
- [9] K. Giannoukou, S. Marelli, and B. Sudret, *A comprehensive framework for multi-fidelity surrogate modelling with noisy data: a gray-box perspective*, Jan. 2024, preprint. [Online]. Available: [https://www.researchgate.net/publication/377527831\\_A\\_COMPREHENSIVE\\_FRAMEWORK\\_FOR\\_MULTI-FIDELITY\\_SURROGATE\\_MODELING\\_WITH\\_NOISY\\_DATA\\_A\\_GRAY-BOX\\_PERSPECTIVE](https://www.researchgate.net/publication/377527831_A_COMPREHENSIVE_FRAMEWORK_FOR_MULTI-FIDELITY_SURROGATE_MODELING_WITH_NOISY_DATA_A_GRAY-BOX_PERSPECTIVE)



- [10] C. V. Mai and B. Sudret, “Surrogate Models for Oscillatory Systems Using Sparse Polynomial Chaos Expansions and Stochastic Time Warping,” *SIAM/ASA Journal on Uncertainty Quantification*, vol. 5, no. 1, pp. 540–571, Jan. 2017.
- [11] G. Matheron, “The intrinsic random functions and their applications,” *Advances in Applied Probability*, 1973.
- [12] B. Echard, N. Gayton, and M. Lemaire, “AK-MCS: An active learning reliability method combining Kriging and Monte Carlo Simulation,” *Structural Safety*, vol. 33, pp. 145–154, Mar. 2011.
- [13] M. Moustapha, S. Marelli, and B. Sudret, “Active learning for structural reliability: survey, general framework and benchmark,” *Structural Safety*, vol. 96, p. 102174, May 2022, arXiv:2106.01713 [stat].
- [14] G. Blatman and B. Sudret, “Adaptive sparse polynomial chaos expansion based on least angle regression,” *Journal of Computational Physics*, vol. 230, pp. 2345–2367, 03 2011.
- [15] S. Marelli and B. Sudret, “UQLab: A Framework for Uncertainty Quantification in Matlab,” in *The 2nd International Conference on Vulnerability and Risk Analysis and Management (ICVRAM 2014)*. University of Liverpool, United Kingdom: American Society of Civil Engineers, 2014, pp. 2554–2563.